Orientation of immobilized antigens on common surfaces by a simple computational model: Exposition of SARS-CoV-2 Spike protein RBD

This is the postprint version of the paper appeared in “Biophysical Chemistry” with doi: 10.1016/j.bpc.2020.106441

Orientation of immobilized antigens on common surfaces by a simple computational model: exposition of SARS-CoV-2 Spike protein RBD epitopes

Linda Cerofolini[1], Marco Fragai[1,2], Claudio Luchinat[1,2], Enrico Ravera[1,2]*

1. Magnetic Resonance Center (CERM) and Interuniversity Consortium for Magnetic Resonance of Metallo Proteins (CIRMMP), Via L. Sacconi 6, 50019 Sesto Fiorentino, Italy

2. Department of Chemistry “Ugo Schiff”, University of Florence, Via della Lastruccia 3, 50019 Sesto Fiorentino, Italy

Keywords

Immunosensing; bioconjugation; united residue model; protein-surface interaction

*Corresponding Author: ravera@cerm.unifi.it

ORCID:

Linda Cerofolini 0000-0002-0795-9594

Marco Fragai 0000-0002-8440-1690

Claudio Luchinat 0000-0003-2271-8921

Enrico Ravera 0000-0001-7708-9208

Abstract

The possibility of immobilizing a protein with antigenic properties on a solid support offers significant possibilities in the development of immunosensors and vaccine formulations. The orientation of the antigen should ensure ready accessibility of the antibodies to the epitope. In this manuscript, we apply a simple computational model to the prediction of the orientation of the receptor binding domain of the SARS-CoV-2 spike protein on surfaces commonly used in lateral-flow devices.

Introduction

The activity and reactivity of an immobilized protein strongly depend on its orientation with respect to a surface. This holds true for enzymes, antibodies and antigens. Therefore, the possibility of to control and manipulate the exposition of the relevant molecular surfaces plays an important role in the rational design of devices based on immobilized proteins. Among these, immunosensors represent an expanding space for research and market opportunities.

While the path to reach a technologically relevant product must rely upon a strong experimental characterization,[1] possibly relying upon atomic-level methodologies,[2–8] it is also true that guidelines for achieving optimal orientations could improve the efficiency of the R&D connected to protein immobilization.[9,10] However, simplified models are not particularly common. In this manuscript we specifically address the problem of determining the orientation of the SARS-CoV-2 Spike protein Receptor Binding Domain (RBD) on a few prototypical surfaces for biomedical use, applying a very simple method based on a united-residue modelling of the protein-surface interactions. This method is based on the works by Jiang, Zhou and del Monte-Martinez,[9,11–17] and encompasses van der Waals and electrostatic interactions, as well as covalent immobilization.

The choice of the target protein is motivated by the recent emergence of a new infectious disease (COVID-19) caused by a coronavirus (SARS-CoV-2).[18] This infectious disease has spread significantly throughout the world, counting 9.266.021 infected people and a death toll of 477.643 as of June 2020,[19] and models suggests that it will remain circulating and active for several months.[20,21] This pandemic outbreak has had a major impact on world economics, with a very long outlook.[22] A capillary control of the diffusion of the infection has proven crucial,[23] and serological tests are expected to have a key role in mass screening.[24,25]

Methods

The structures of the proteins were downloaded from the PDB,[26] the pKa values of reactive groups were calculated using PROPKA,[27,28] and the interfaces were calculated using the PDBe PISA server.[29] The non-bonded interaction of a residue of type i is represented with a Lennard-Jones (LJ) potential:[13]

$$U(r) = 4\varepsilon_i \left[\left(\frac{\sigma_i}{r + \delta_i} \right)^{12} - \left(\frac{\sigma_i}{r + \delta_i} \right)^{6} \right]$$

where r is the nearest distance between the residue and the surface, $\varepsilon_i$is the energy at the minimum position, $\sigma_i$is the equivalent van der Waals radius of each residue and δ_i is a size parameter taken from the literature (see tables S2-S7).

The electrostatic interaction is represented through the Gouy-Chapman potential[13,30]

$$U(r) = \frac{\sigma_S q_i e^{-\kappa r}}{\kappa \varepsilon_r \varepsilon_0}$$

where r is the nearest distance between the i-th residue with charge q_i and the surface, σ_S is the surface charge density, κ is the inverse Debye Length calculated from the ionic strength I as $\kappa^{-1} = 0.304/\sqrt{I}$, and the relative permittivity of the medium is assumed to be distance-dependent ($\varepsilon_r = r$).[13,30] A 1:1 buffer salt concentration of 0.15 mol dm^{-3} is assumed.

For silica, the surface charge density is estimated to be -0.3 C m^{-2}.[31]

For self-assembled charged monolayers, the charge density is set to +/-0.02 C m^{-2}.[12,17]

The formation of a covalent bond is treated with the following potential:

$$U(r) = \begin{cases} \varepsilon_B \; if \; r \leq \sigma_i \\ 0 \; elsewhere \end{cases}$$

where ε_B is the bond energy and is set to 600 kJ mol^{-1} for imino bonds[32] and 100 kJ mol^{-1} for gold-thiol bonds,[33–35] regardless of the starting oxidation state of the thiol.[36] The desolvation energy is already accounted for in the vdW term.

LJ parameters for epoxide-glyoxyl functionalization is assumed to be equal to SAM-CO_2H, whereas for gold the parameters have been adapted from reference [37].

The sampling of the relative protein-surface orientations is performed by rotating a plane around the center of mass of the protein. The plane is initially parallel to the z=0 plane. Only two rotations are necessary, as all the rotations around the normal to the plane will yield the same energy. The first rotation by an angle $\alpha \in [0, \pi]$ is applied around the y-axis, followed by another rotation of an angle $\beta \in [0, 2\pi]$ around the z-axis, and then a translation is applied to optimize the position, similarly to what is done in the popular PALES software.[38–40] The sampling of the α, β pairs is made uniform by using REPULSION angular sampling.[41–43] The distance of the plane to the protein is then set by minimizing the energy terms described above.

Results and discussion

The orientation of the antigen with respect to the surface must ensure the accessibility of the epitope to the antibodies, to guarantee the recognition. Therefore, we have selected the crystallographic structure of RBD in complex with a fragment (FAB) of the human antibody CR3022 (PDB ID: 6W41),[44] and identified the relevant interface residues (Figure 1 and Table S1). In the analysis, we assume that the full length antibody will have the same accessibility as the FAB because of the high flexibility of the linkers of the heavy chains (see figure S1).[45–48] While the spike protein is highly glycosylated at N- and O-positions,[49,50] the structured part of the RBD which is recognized by the antibody only carries a glycation at position 343[49] (pink in figure 1), which faces away from the antibody binding site, therefore we have not considered glycation (experimentally, this would be done expressing recombinant RBD in prokaryotic cells, whereas glycation is obtained in human cells[49]).

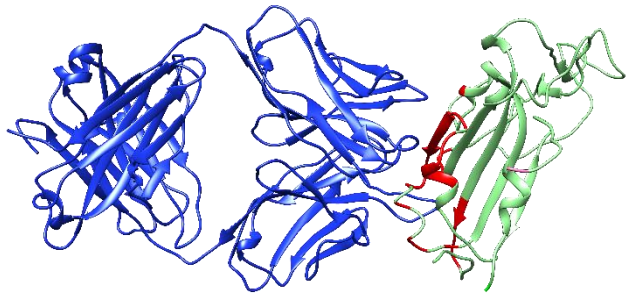

Figure 1. Biological assembly from the crystallographic structure 6W41. The SARS-CoV-2 receptor binding domain is shown in light green, with the interacting residues highlighted in red and the N-terminus highlighted in green. The glycation site 343 is highlighted in pink. The fragment of the human antibody CR3022 is shown in blue.

Interaction with a hydrophobic surface

Hydrophobic adsorption is the selective adsorption on hydrophobic carriers at low ionic strength.[51] It is a rather common immobilization protocol, because of its simplicity. The interaction is here represented only through a simple Lennard-Jones (LJ) potential, the parameters of which have been defined according to the hydrophobicity index (table

S2).[37,52–54] The most probable orientation is shown in figure 2, with the surface represented as a disk. In this, and in the following representations, the interaction is calculated for the antigen alone, and then the complex is shown for examining the interference of the surface with the binding. Most of the orientations with higher probability involve contacts between the interface residues and the surface, and are therefore expected to be poorly efficient for the recognition. This is not completely unexpected; as hydrophobic carriers mimic the interfaces formed by the naturally occurring interfaces of the proteins.

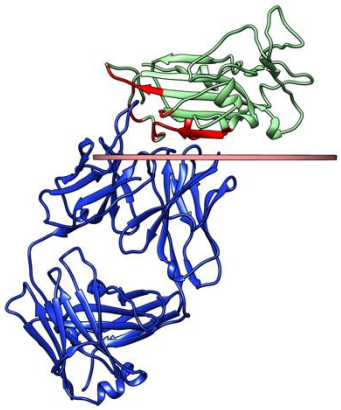

Figure 2. Antigen-FAB complex shown in superposition with the most probable positioning of a hydrophobic surface. The surface is represented as a disk, aligned with the viewer.

Interaction with charged surfaces

The electrostatic interaction of the i-th residue with the uniformly charged surface with a given charge density is estimated by the Gouy-Chapman potential,[11,13] which is added to a LJ term. The parameters defining each system are listed in tables S3-S6.

We have considered the following surfaces:

1) silica - a common chromatographic support with high negative surface charge;

2) positively charged self-assembled monolayer (SAM), with amino capping of the chains;[12,17]

3) negatively charged SAM, with carboxylic capping of the chains.[12,17]

Supports #2 and #3 imply the possibility of colorimetric detection through gold,[55] vide infra. The most probable orientations are shown in figure 3.

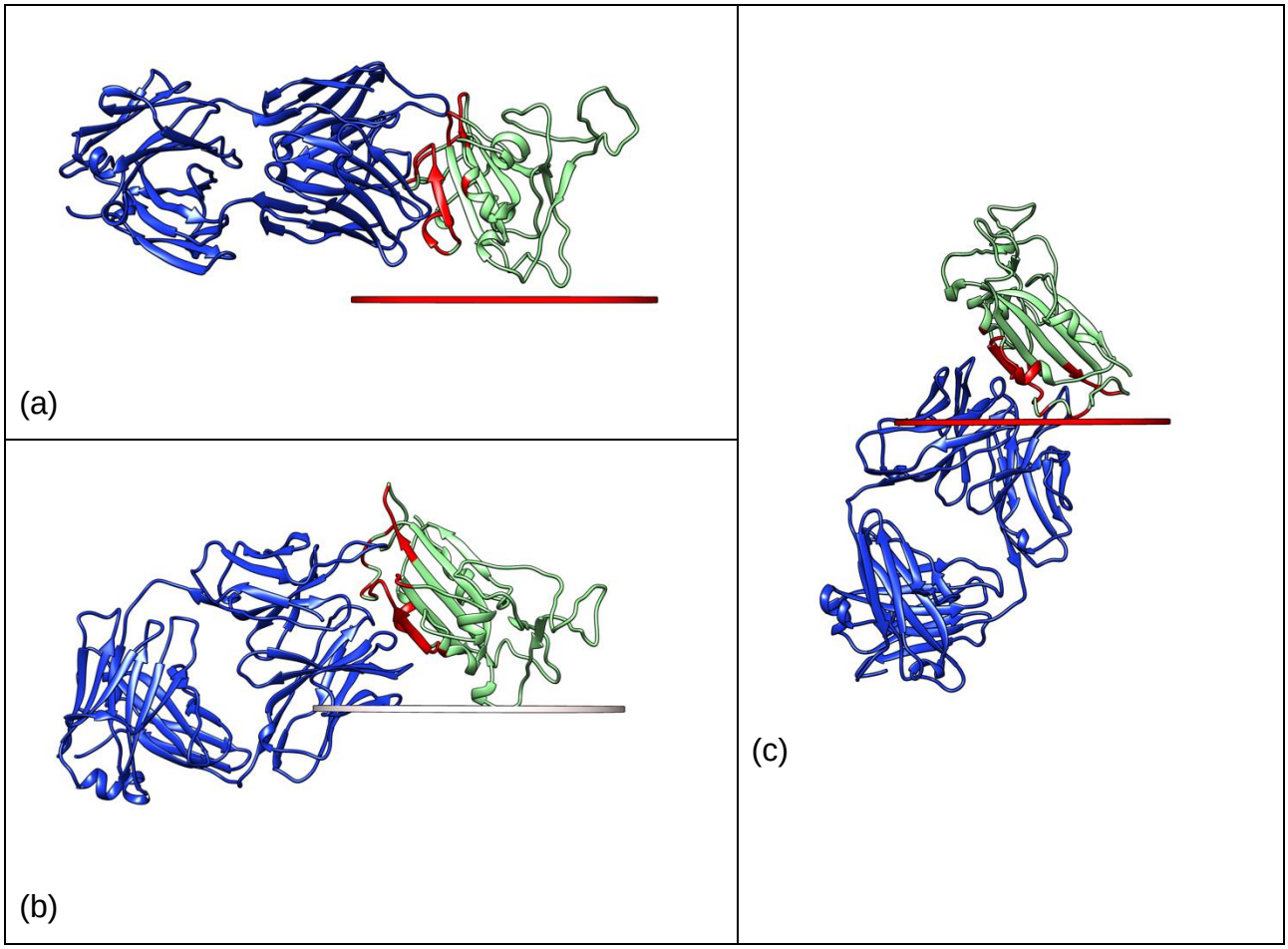

Figure 3. Antigen-FAB complex shown in superposition with the most probable positioning with respect to charged surfaces: (a) silica, (b) negatively charged SAM and (c) positively charged SAM.

It is apparent that only negatively charged surfaces allow for the exposition of the epitope, and this is anyway relatively marginal. Therefore, our analysis suggests that it would be nontrivial to achieve a good orientation relying upon adsorption.

On these grounds, we have considered directed approaches based on stronger interactions. In particular, we have considered epoxide-glyoxyl (directed at primary amine moieties)[56] and gold (thiols and disulfide bridges).[55]

The glyoxyl-based approach is quite popular for multipoint orientation-selective immobilization of proteins on surfaces. It involves a two-step mechanism, in the first step, the primary amine groups of the protein are allowed to react with the aldehyde groups to form Schiff base bonds, in the second step the bonds are reduced with sodium borohydride.

This kind of immobilization has been simulated in a similar way as described by del Monte-Martìnez et al.,[10] assuming a working pH = 7.5, to maximize the reactivity of the N-terminus and at the same time limiting the reactivity of lysine residues (see table S7).
The choice of gold is also extremely popular, because of two reasons: the strong plasmonic response of gold, which causes a purple coloring of the bioconjugate, and because of the relatively easy manipulation required. Current SARS-CoV2 serological tests are indeed based on gold conjugates.[57] The conjugation to the surface is simulated in the same way as the amine-glyoxyl reaction, assuming that all cysteines are equally reactive towards gold (disulfide bridges can interact with gold to a comparable extent as thiols).[36] Colloidal gold has a net negative surface charge,[58] but including the electrostatic term has no impact on the recovered conformations.

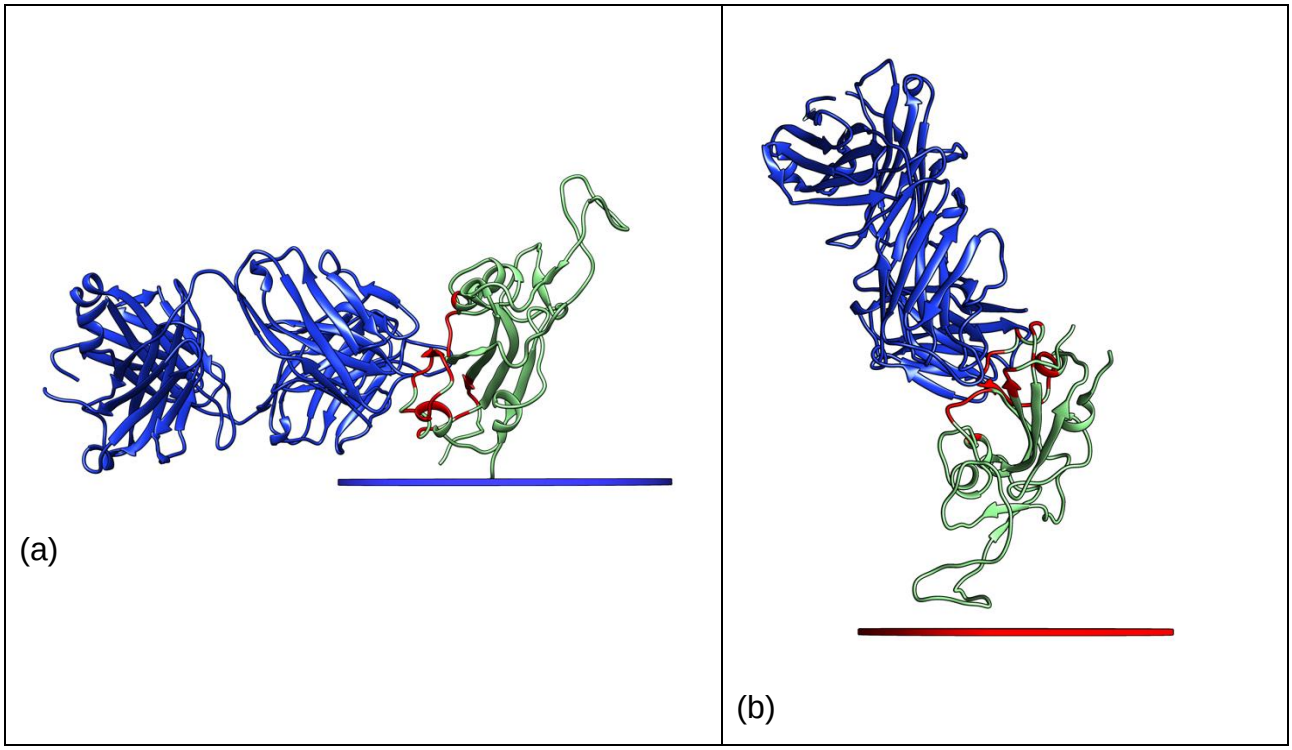

Figure 4. Antigen-FAB complex shown in superposition with the most probable positioning with respect to covalently bound surfaces (a) epoxide-glyoxyl and (b) gold.

In the epoxide-glyoxyl strategy, the conjugation appears to be mostly directed at the N-terminus, which is facing away from the recognition interface but is not topologically very

remote. Therefore, the epitope will only be partially exposed, whereas for the gold conjugation, ample access to the epitope is possible in the most probable orientation.

Finally, a completely different strategy could be applied for conjugation to (e.g.) gold nanoparticles: the use of a avidin-biotin affinity system.[59] Biotinylation can be achieved through amine-specific reagents,[60] and improvement in the selectivity can be achieved with minimal engineering of the sequence.[61] Given that there is a rather substantial difference in the calculated pKas for the different amine sites (see table S7), it can be expected that, for pH values lower than 7, all lysine residues will be protonated and thus less reactive with probability higher than 99%. The N-terminus is not facing the interaction site (see figure 1). Therefore, selective biotinylation at the N-terminus is expected to be possible. In this case, the accessibility of the epitope is warranted if the interaction between the antigen and streptavidin, if at all possible, is sufficiently weak.
To explore this possibility we have performed an initial-stage docking using ZDOCK,[62] and inspected the first two elements that had a significantly higher ZDOCK score (Figure S2). The possible interaction between the RBD and streptavidin was investigated also using HADDOCK2.4.[63] The protein-protein interface residues were predicted with CPORT,[64] and then used as “active” and “passive” residues in the HADDOCK calculation. About 10 lowly populated clusters with weak energy were obtained; the most significant three with the lowest HADDOCK-scores are reported in Figure S3 and their energies in Table S8. Both dockings indicate that, should the interaction occur, it would occur in a position that does not interfere with the antigen-antibody recognition.

In conclusion, we propose that very simple modelling approaches can provide hints towards how to orient antigens in a way to maximize the exposition of epitopes, and therefore help in the initial moments of the design of conjugates for immunologic applications. This simple modelling can, for instance, explain why random conjugation of the RBD to a gold surface yields responsive immunosensors. An experimental verification of our prediction by means of solid-state NMR[3,6–8,65–67] is being started in our lab. Overall, the expected short-time impact of our work is to provide guidelines to avoid the experimental exploration of immobilization pathways that are less promising.

Acknowledgements

Discussion with Luca Sgheri (National Research Council of Italy) and Cesare Bracco (Department of Mathematics and Informatics “Ulisse Dini”, University of Florence) is acknowledged. This work has been supported by the Fondazione Cassa di Risparmio di Firenze, the Italian Ministero della Salute through the grant GR- 2016-02361586, the Italian Ministero dell’Istruzione, dell’Università e della Ricerca through the “Progetto Dipartimenti di Eccellenza 2018-2022” to the Department of Chemistry “Ugo Schiff” of the University of Florence, and the University of Florence through the “Progetti Competitivi per Ricercatori”. The authors acknowledge the support and the use of resources of Instruct-ERIC, a landmark ESFRI project, and specifically the CERM/CIRMMP Italy center.

References

[1] J.M. Bolivar, I. Eisl, B. Nidetzky, Advanced characterization of immobilized enzymes as heterogeneous biocatalysts, Catal. Today. 259 (2016) 66–80. https://doi.org/10.1016/j.cattod.2015.05.004.

[2] Matlahov, I., Geiger, Y., Goobes, G., Trapping RNase A on MCM41 pores: effects on structure stability, product inhibition and overall enzymatic activity, Phys. Chem. Chem. Phys. 16 (2014) 9031–9038.

[3] K.H. Mroue, Y. Nishiyama, M. Kumar Pandey, B. Gong, E. McNerny, D.H. Kohn, M.D. Morris, A. Ramamoorthy, Proton-Detected Solid-State NMR Spectroscopy of Bone with Ultrafast Magic Angle Spinning, Sci. Rep. 5 (2015) 11991. https://doi.org/10.1038/srep11991.

[4] S. Varghese, P.J. Halling, D. Häussinger, S. Wimperis, High-Resolution Structural Characterization of a Heterogeneous Biocatalyst Using Solid-State NMR, J. Phys. Chem. C. 120 (2016) 28717–28726. https://doi.org/10.1021/acs.jpcc.6b11575.

[5] D. Tian, T. Li, R. Zhang, Q. Wu, T. Chen, P. Sun, A. Ramamoorthy, Conformations and Intermolecular Interactions in Cellulose/Silk Fibroin Blend Films: A Solid-State NMR Perspective, J. Phys. Chem. B. 121 (2017) 6108–6116. https://doi.org/10.1021/acs.jpcb.7b02838.

[6] N. Adiram-Filiba, A. Schremer, E. Ohaion, M. Nadav-Tsubery, T. Lublin-Tennenbaum, K. Keinan-Adamsky, G. Goobes, Ubiquitin immobilized on mesoporous MCM41 silica surfaces - Analysis by solid-state NMR with biophysical and surface characterization, Biointerphases. 12 (2017) 02D414. https://doi.org/10.1116/1.4983273.

[7] A. Louka, I. Matlahov, S. Giuntini, L. Cerofolini, A. Cavallo, S. Pillozzi, E. Ravera, M. Fragai, A. Arcangeli, A. Ramamoorthy, G. Goobes, C. Luchinat, Engineering l-asparaginase for spontaneous formation of calcium phosphate bioinspired microreactors, Phys. Chem. Chem. Phys. PCCP. 20 (2018) 12719–12726. https://doi.org/10.1039/c8cp00419f.

[8] L. Cerofolini, S. Giuntini, E. Ravera, C. Luchinat, F. Berti, M. Fragai, Structural characterization of a protein adsorbed on aluminum hydroxide adjuvant in vaccine formulation, Npj Vaccines. 4 (2019) 1–5. https://doi.org/10.1038/s41541-019-0115-7.

[9] B. Cutiño-Avila, D. Gil Pradas, C. Aragón Abreu, Y. Fernández Marrero, M. Hernández de la Torre, E. Salas Sarduy, M. de los Á. Chávez Planes, J.M. Guisán Seijas, J. Díaz Brito, A. del Monte-Martínez, Computer-aided design of bromelain and papain covalent immobilization,

Rev. Colomb. Biotecnol. 16 (2014) 19–28. https://doi.org/10.15446/rev.colomb.biote.v16n1.44184.
[10] A. del Monte-Martínez, B.V. Cutiño-Avila, J. González-Bacerio, Rational Design Strategy as a Novel Immobilization Methodology Applied to Lipases and Phospholipases, in: G. Sandoval (Ed.), Lipases Phospholipases Methods Protoc., Springer, New York, NY, 2018: pp. 243–283. https://doi.org/10.1007/978-1-4939-8672-9_14.
[11] J. Zhou, S. Chen, S. Jiang, Orientation of Adsorbed Antibodies on Charged Surfaces by Computer Simulation Based on a United-Residue Model, Langmuir. 19 (2003) 3472–3478. https://doi.org/10.1021/la026871z.
[12] J. Zhou, J. Zheng, S. Jiang, Molecular Simulation Studies of the Orientation and Conformation of Cytochrome c Adsorbed on Self-Assembled Monolayers, J. Phys. Chem. B. 108 (2004) 17418–17424. https://doi.org/10.1021/jp038048x.
[13] Y. Xie, J. Zhou, S. Jiang, Parallel tempering Monte Carlo simulations of lysozyme orientation on charged surfaces, J. Chem. Phys. 132 (2010) 065101. https://doi.org/10.1063/1.3305244.
[14] J. Liu, C. Liao, J. Zhou, Multiscale Simulations of Protein G B1 Adsorbed on Charged Self-Assembled Monolayers, Langmuir. 29 (2013) 11366–11374. https://doi.org/10.1021/la401171v.
[15] C. Liao, Y. Xie, J. Zhou, Computer simulations of fibronectin adsorption on hydroxyapatite surfaces, RSC Adv. 4 (2014) 15759–15769. https://doi.org/10.1039/C3RA47381C.
[16] D. Zhao, C. Peng, J. Zhou, Lipase adsorption on different nanomaterials: a multi-scale simulation study, Phys. Chem. Chem. Phys. 17 (2014) 840–850. https://doi.org/10.1039/C4CP04696J.
[17] J. Liu, G. Yu, J. Zhou, Ribonuclease A adsorption onto charged self-assembled monolayers: A multiscale simulation study, Chem. Eng. Sci. 121 (2015) 331–339. https://doi.org/10.1016/j.ces.2014.07.021.
[18] WHO Statement Regarding Cluster of Pneumonia Cases in Wuhan, China, (n.d.). https://www.who.int/china/news/detail/09-01-2020-who-statement-regarding-cluster-of-pneumonia-cases-in-wuhan-china (accessed May 11, 2020).
[19] E. Dong, H. Du, L. Gardner, An interactive web-based dashboard to track COVID-19 in real time, Lancet Infect. Dis. 20 (2020) 533–534. https://doi.org/10.1016/S1473-3099(20)30120-1.
[20] D. Fanelli, F. Piazza, Analysis and forecast of COVID-19 spreading in China, Italy and France, Chaos Solitons Fractals. 134 (2020) 109761. https://doi.org/10.1016/j.chaos.2020.109761.
[21] T. Carletti, D. Fanelli, F. Piazza, COVID-19: The unreasonable effectiveness of simple models, ArXiv200511085 Phys. Q-Bio. (2020). http://arxiv.org/abs/2005.11085 (accessed June 28, 2020).
[22] EU/EA measures to mitigate the economic, financial and social effects of coronavirus, (n.d.) 24.
[23] E. Lavezzo, E. Franchin, C. Ciavarella, G. Cuomo-Dannenburg, L. Barzon, C.D. Vecchio, L. Rossi, R. Manganelli, A. Loregian, N. Navarin, D. Abate, M. Sciro, S. Merigliano, E. Decanale, M.C. Vanuzzo, F. Saluzzo, F. Onelia, M. Pacenti, S. Parisi, G. Carretta, D. Donato, L. Flor, S. Cocchio, G. Masi, A. Sperduti, L. Cattarino, R. Salvador, K.A.M. Gaythorpe, I.C.L.C.-19 R. Team, A.R. Brazzale, S. Toppo, M. Trevisan, V. Baldo, C.A. Donnelly, N.M. Ferguson, I. Dorigatti, A. Crisanti, Suppression of COVID-19 outbreak in the municipality of Vo, Italy, MedRxiv. (2020) 2020.04.17.20053157. https://doi.org/10.1101/2020.04.17.20053157.
[24] A.K. Winter, S.T. Hegde, The important role of serology for COVID-19 control, Lancet Infect. Dis. 0 (2020). https://doi.org/10.1016/S1473-3099(20)30322-4.

[25] Y. Eliaz, M. Danovich, G.P. Gasic, Poolkeh Finds the Optimal Pooling Strategy for a Population-wide COVID-19 Testing (Israel, UK, and US as Test Cases), MedRxiv. (2020) 2020.04.25.20079343. https://doi.org/10.1101/2020.04.25.20079343.
[26] H.M. Berman, J. Westbrook, Z. Feng, G. Gilliland, T.N. Bhat, H. Weissig, I.N. Shindyalov, P.E. Bourne, The Protein Data Bank, Nucleic Acids Res. 28 (2000) 235–242. https://doi.org/10.1093/nar/28.1.235.
[27] H. Li, A.D. Robertson, J.H. Jensen, Very fast empirical prediction and rationalization of protein pKa values, Proteins. 61 (2005) 704–721. https://doi.org/10.1002/prot.20660.
[28] C.R. Søndergaard, M.H.M. Olsson, M. Rostkowski, J.H. Jensen, Improved Treatment of Ligands and Coupling Effects in Empirical Calculation and Rationalization of pKa Values, J. Chem. Theory Comput. 7 (2011) 2284–2295. https://doi.org/10.1021/ct200133y.
[29] E. Krissinel, K. Henrick, Inference of Macromolecular Assemblies from Crystalline State, J. Mol. Biol. 372 (2007) 774–797. https://doi.org/10.1016/j.jmb.2007.05.022.
[30] H.-K. Tsao, Electrostatic Interactions of a String-Like Particle with a Charged Plate, J. Colloid Interface Sci. 202 (1998) 527–540. https://doi.org/10.1006/jcis.1998.5471.
[31] G. Yu, J. Zhou, Understanding the curvature effect of silica nanoparticles on lysozyme adsorption orientation and conformation: a mesoscopic coarse-grained simulation study, Phys. Chem. Chem. Phys. 18 (2016) 23500–23507. https://doi.org/10.1039/C6CP01478J.
[32] P.W. Atkins, J.D. Paula, J. Keeler, Atkins' Physical Chemistry, Oxford University Press, 2018.
[33] D.M. Collard, M.Anne. Fox, Use of electroactive thiols to study the formation and exchange of alkanethiol monolayers on gold, Langmuir. 7 (1991) 1192–1197. https://doi.org/10.1021/la00054a029.
[34] H. Häkkinen, The gold–sulfur interface at the nanoscale, Nat. Chem. 4 (2012) 443–455. https://doi.org/10.1038/nchem.1352.
[35] Y. Xue, X. Li, H. Li, W. Zhang, Quantifying thiol–gold interactions towards the efficient strength control, Nat. Commun. 5 (2014) 1–9. https://doi.org/10.1038/ncomms5348.
[36] H. Grönbeck, A. Curioni, W. Andreoni, Thiols and Disulfides on the Au(111) Surface: The Headgroup−Gold Interaction, J. Am. Chem. Soc. 122 (2000) 3839–3842. https://doi.org/10.1021/ja993622x.
[37] G. Brancolini, H. Lopez, S. Corni, V. Tozzini, Low-Resolution Models for the Interaction Dynamics of Coated Gold Nanoparticles with β2-microglobulin, Int. J. Mol. Sci. 20 (2019) 3866. https://doi.org/10.3390/ijms20163866.
[38] M. Zweckstetter, A. Bax, Prediction of Sterically Induced Alignment in a Dilute Liquid Crystalline Phase: Aid to Protein Structure Determination by NMR, J. Am. Chem. Soc. 122 (2000) 3791–3792. https://doi.org/10.1021/ja0000908.
[39] M. Zweckstetter, G. Hummer, A. Bax, Prediction of charge-induced molecular alignment of biomolecules dissolved in dilute liquid-crystalline phases, Biophys. J. 86 (2004) 3444–3460. https://doi.org/10.1529/biophysj.103.035790.
[40] M. Zweckstetter, NMR: prediction of molecular alignment from structure using the PALES software, Nat. Protoc. 3 (2008) 679–690. https://doi.org/10.1038/nprot.2008.36.
[41] null Bak, null Nielsen, REPULSION, A Novel Approach to Efficient Powder Averaging in Solid-State NMR, J. Magn. Reson. San Diego Calif 1997. 125 (1997) 132–139. https://doi.org/10.1006/jmre.1996.1087.
[42] M. Bak, J.T. Rasmussen, N.C. Nielsen, SIMPSON: A General Simulation Program for Solid-State NMR Spectroscopy, J. Magn. Reson. 147 (2000) 296–330.
[43] Z. Tošner, R. Andersen, B. Stevensson, M. Edén, N.Chr. Nielsen, T. Vosegaard, Computer-intensive simulation of solid-state NMR experiments using SIMPSON, J. Magn. Reson. 246 (2014) 79–93. https://doi.org/10.1016/j.jmr.2014.07.002.

[44] M. Yuan, N.C. Wu, X. Zhu, C.-C.D. Lee, R.T.Y. So, H. Lv, C.K.P. Mok, I.A. Wilson, A highly conserved cryptic epitope in the receptor-binding domains of SARS-CoV-2 and SARS-CoV, Science. (2020). https://doi.org/10.1126/science.abb7269.
[45] L.J. Harris, S.B. Larson, K.W. Hasel, A. McPherson, Refined Structure of an Intact IgG2a Monoclonal Antibody, Biochemistry. 36 (1997) 1581–1597. https://doi.org/10.1021/bi962514+.
[46] L.J. Harris, E. Skaletsky, A. McPherson, Crystallographic structure of an intact IgG1 monoclonal antibody11Edited by I. A. Wilson, J. Mol. Biol. 275 (1998) 861–872. https://doi.org/10.1006/jmbi.1997.1508.
[47] E.O. Saphire, P.W.H.I. Parren, R. Pantophlet, M.B. Zwick, G.M. Morris, P.M. Rudd, R.A. Dwek, R.L. Stanfield, D.R. Burton, I.A. Wilson, Crystal Structure of a Neutralizing Human IgG Against HIV-1: A Template for Vaccine Design, Science. 293 (2001) 1155–1159. https://doi.org/10.1126/science.1061692.
[48] G. Scapin, X. Yang, W.W. Prosise, M. McCoy, P. Reichert, J.M. Johnston, R.S. Kashi, C. Strickland, Structure of full-length human anti-PD1 therapeutic IgG4 antibody pembrolizumab, Nat. Struct. Mol. Biol. 22 (2015) 953–958. https://doi.org/10.1038/nsmb.3129.
[49] A. Shajahan, N.T. Supekar, A.S. Gleinich, P. Azadi, Deducing the N- and O-glycosylation profile of the spike protein of novel coronavirus SARS-CoV-2, Glycobiology. (n.d.). https://doi.org/10.1093/glycob/cwaa042.
[50] A.C. Walls, Y.-J. Park, M.A. Tortorici, A. Wall, A.T. McGuire, D. Veesler, Structure, Function, and Antigenicity of the SARS-CoV-2 Spike Glycoprotein, Cell. 181 (2020) 281-292.e6. https://doi.org/10.1016/j.cell.2020.02.058.
[51] B. Al-Duri, E. Robinson, S. McNerlan, P. Bailie, Hydrolysis of edible oils by lipases immobilized on hydrophobic supports: Effects of internal support structure, J. Am. Oil Chem. Soc. 72 (1995) 1351–1359. https://doi.org/10.1007/BF02546211.
[52] S. Miyazawa, R.L. Jernigan, Residue-residue potentials with a favorable contact pair term and an unfavorable high packing density term, for simulation and threading, J. Mol. Biol. 256 (1996) 623–644. https://doi.org/10.1006/jmbi.1996.0114.
[53] T. Bereau, M. Deserno, Generic coarse-grained model for protein folding and aggregation, J. Chem. Phys. 130 (2009) 235106. https://doi.org/10.1063/1.3152842.
[54] Y.C. Kim, G. Hummer, Coarse-grained models for simulations of multiprotein complexes: application to ubiquitin binding, J. Mol. Biol. 375 (2008) 1416–1433. https://doi.org/10.1016/j.jmb.2007.11.063.
[55] M.-E. Aubin-Tam, Conjugation of Nanoparticles to Proteins, in: P. Bergese, K. Hamad-Schifferli (Eds.), Nanomater. Interfaces Biol. Methods Protoc., Humana Press, Totowa, NJ, 2013: pp. 19–27. https://doi.org/10.1007/978-1-62703-462-3_3.
[56] F. López-Gallego, G. Fernandez-Lorente, J. Rocha-Martin, J.M. Bolivar, C. Mateo, J.M. Guisan, Stabilization of enzymes by multipoint covalent immobilization on supports activated with glyoxyl groups, Methods Mol. Biol. Clifton NJ. 1051 (2013) 59–71. https://doi.org/10.1007/978-1-62703-550-7_5.
[57] Z. Li, Y. Yi, X. Luo, N. Xiong, Y. Liu, S. Li, R. Sun, Y. Wang, B. Hu, W. Chen, Y. Zhang, J. Wang, B. Huang, Y. Lin, J. Yang, W. Cai, X. Wang, J. Cheng, Z. Chen, K. Sun, W. Pan, Z. Zhan, L. Chen, F. Ye, Development and clinical application of a rapid IgM-IgG combined antibody test for SARS-CoV-2 infection diagnosis, J. Med. Virol. n/a (n.d.). https://doi.org/10.1002/jmv.25727.
[58] R.R. Kumal, T.E. Karam, L.H. Haber, Determination of the Surface Charge Density of Colloidal Gold Nanoparticles Using Second Harmonic Generation, J. Phys. Chem. C. 119 (2015) 16200–16207. https://doi.org/10.1021/acs.jpcc.5b00568.

[59] C. Oliver, Colloidal gold/streptavidin methods, Methods Mol. Biol. Clifton NJ. 588 (2010) 375–380. https://doi.org/10.1007/978-1-59745-324-0_40.
[60] I. Sélo, L. Négroni, C. Créminon, J. Grassi, J.M. Wal, Preferential labeling of α-amino N-terminal groups in peptides by biotin: application to the detection of specific anti-peptide antibodies by enzyme immunoassays, J. Immunol. Methods. 199 (1996) 127–138. https://doi.org/10.1016/S0022-1759(96)00173-1.
[61] M.C. Martos-Maldonado, C.T. Hjuler, K.K. Sørensen, M.B. Thygesen, J.E. Rasmussen, K. Villadsen, S.R. Midtgaard, S. Kol, S. Schoffelen, K.J. Jensen, Selective N-terminal acylation of peptides and proteins with a Gly-His tag sequence, Nat. Commun. 9 (2018). https://doi.org/10.1038/s41467-018-05695-3.
[62] B.G. Pierce, K. Wiehe, H. Hwang, B.-H. Kim, T. Vreven, Z. Weng, ZDOCK server: interactive docking prediction of protein-protein complexes and symmetric multimers, Bioinforma. Oxf. Engl. 30 (2014) 1771–1773. https://doi.org/10.1093/bioinformatics/btu097.
[63] G.C.P. van Zundert, J.P.G.L.M. Rodrigues, M. Trellet, C. Schmitz, P.L. Kastritis, E. Karaca, A.S.J. Melquiond, M. van Dijk, S.J. de Vries, A.M.J.J. Bonvin, The HADDOCK2.2 Web Server: User-Friendly Integrative Modeling of Biomolecular Complexes, J. Mol. Biol. 428 (2016) 720–725. https://doi.org/10.1016/j.jmb.2015.09.014.
[64] S.J. de Vries, A.M.J.J. Bonvin, CPORT: A Consensus Interface Predictor and Its Performance in Prediction-Driven Docking with HADDOCK, PLOS ONE. 6 (2011) e17695. https://doi.org/10.1371/journal.pone.0017695.
[65] S. Giuntini, L. Cerofolini, E. Ravera, M. Fragai, C. Luchinat, Atomic structural details of a protein grafted onto gold nanoparticles, Sci. Rep. 7 (2017) 17934. https://doi.org/10.1038/s41598-017-18109-z.
[66] E. Ravera, L. Cerofolini, T. Martelli, A. Louka, M. Fragai, C. Luchinat, 1H-detected solid-state NMR of proteins entrapped in bioinspired silica: a new tool for biomaterials characterization, Sci. Rep. 6 (2016) 27851.
[67] R. Huang, K. Yamamoto, M. Zhang, N. Popovych, I. Hung, S.-C. Im, Z. Gan, L. Waskell, A. Ramamoorthy, Probing the Transmembrane Structure and Dynamics of Microsomal NADPH-cytochrome P450 oxidoreductase by Solid-State NMR, Biophys. J. 106 (2014) 2126–2133. https://doi.org/10.1016/j.bpj.2014.03.051.